MEMOIRS OF THE SCHOOL OF ENGINEERING, OKAYAMA UNIVERSITY, Vol. 1, No. 1, MARCH, 1966

The RC Network Analyzer Using the High Permittivity Ceramics and its Applications

Takayoshi MISAKI and Osamu KATO

Department of Electrical Engineering, Okayama University

(Received November 20, 1965)

Described in this paper are the design considerations of the simple element of the two-dimensional RC distributed constant circuit and its applications for the analysis of the transient heat conduction problems in engineering work. This element is formed by coating with the resistive film the upper surface of the high permittivity ceramics plate whose back side to be silvered. In addition to a resistivity of every elementary area within the resistive film, there exists capacitive coupling between the area and ground. This element can be regarded as a typical two-dimensional RC distributed system and utilized as a simulator for the same dimensional heat conduction system. It has a convenience and high accuracy for the analysis of the transient heat conduction problems in engineering work.

§ 1. Introduction

The simulation of the diffusion equation by electrical means can be accomplished with the resistance and the capacitance. The RC network element described in this paper is a simple and typical two-dimensional RC distributed constant circuit and has an accuracy good enough as the simulator of the diffusion equation. In practice, it may be utilized for the analysis of the two-dimensional heat conduction problems in engineering work.

§ 2. Structure of the element

A cross-sectional view of the element is shown in Fig. 1.

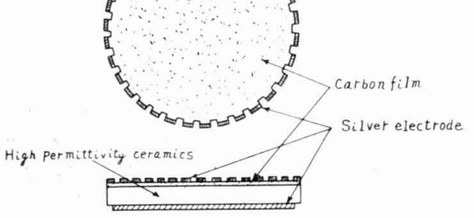

Fig. 1. A cross-sectional view of the element

The base plate of the element is formed by the high permittivity ceramics, such as, TiO_2 or $BaTiO_3$. Both surfaces of the plate are sufficiently polished up.

It is coated one side with a carbon film and the other side with a layer of silver paint.

There exists capacitive coupling between every point along the carbon film having uniform resistivity and the silver electrode. Silver paint is also preferred as the electrode material for boundaries. The shape of the desired boundary is painted on the carbon film, and can be repainted in accordance with the problems. The accuracy of such a element is determined in the main by thickness variation of the base plate. In general, the magnitude of the capacitance per unit area is proportional to the permittivity and inverse proportional to the thickness of the dielectric material. Here as the plate of this element is formed by the high permittivity ceramics, it is not necessary to be made the plate thin specially. For instance, in the case of the TiO_2 plate, the element whose thickness is $3.4\,mm$, has the capacitance per unit area of

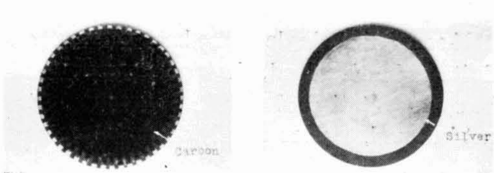

Fig. 2. A sample of the element using the titanium dioxide ceramics

$25\,pF/cm^2$. Accordingly, the thickness variation of the element can be decreased enough. A sample is shown in Fig. 2.

§ 3. Measurement of the circuit constants of the element

The electrical resistance in one specific direction across opposite extremities of area (R_o) and

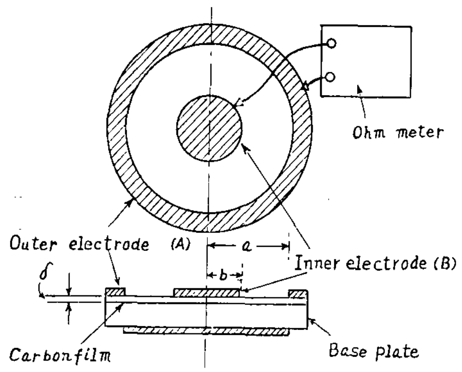

Fig. 3. The measuring circuit of the electrical resistance per unit square (R_0) of the element

the electrical capacitance per unit area (C_0) are measured conveniently as follows.

As shown in Fig. 3, a pair of electrode is set up and the electrical resistance between both electrodes (R_a) is measured by ohm meter. Determing the resistance R_a, the resistance R_o is given by

$$R_0 = \frac{2\pi R_a}{ln(a/b)} \quad (\Omega) \tag{1}$$

where a = inner radius of electrode (A) (cm)
b = radius of electrode (B) (cm)

Also the capacitance C_0 is given by

$$C_0 = \frac{\varepsilon_0 \varepsilon_s}{d} \quad (F/cm^2) \tag{2}$$

where ε_0 = permittivity of free space
ε_s = electric permittivity
d = dielectric thickness (cm)

Therefore C_0 is determined by substituting the measured value of the dielectric thickness d into Eq. (2).

Measuring results of some samples of the element are shown in Table 1.

Table 1. Measuring results of samples

Sample	Ceramics	ε_s	Diameter (mm)	Thickness (mm)	C_0 (pF/cm^2)	R_0 ($k\Omega$)	S (cm^2)
A	$BaTiO_3$	1,500	53	2.0	660	1	16.6
B	TiO_2	100	120	3.4	26	105	1,140

§ 4. The analog approach

The imaginary equivalent circuit of the element is shown in Fig. 4.

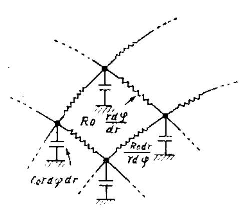

Fig. 4. The imaginary equivalent circuit of the element

In cylindrical coordinates, this circuit is governed by

$$-\frac{\partial v}{\partial r} = R_0 i_r \tag{3}$$

$$-\frac{\partial v}{r\partial\varphi} = R_0 i_\varphi \tag{4}$$

$$\frac{i_r}{r} + \frac{\partial i_r}{\partial r} + \frac{1}{r}\frac{\partial i_\varphi}{\partial\varphi} = -C_0\frac{\partial v}{\partial t} \tag{5}$$

These equations can be reformulated as

$$\frac{1}{r}\frac{\partial}{\partial r}\left(r\frac{\partial v}{\partial r}\right) + \frac{1}{r^2}\frac{\partial^2 v}{\partial\varphi^2} = R_0 C_0 \frac{\partial v}{\partial t} \tag{6}$$

Heat flow in a two-dimensional field is governed by

$$\frac{1}{R}\frac{\partial}{\partial R}\left(R\frac{\partial\theta}{\partial R}\right) + \frac{1}{R^2}\frac{\partial^2\theta}{\partial\varphi^2} = \frac{c\rho}{\eta}\frac{\partial\theta}{\partial\tau} \tag{7}$$

For evey term in Eq. (6) there is a corresponding term of the same order of differentiation in Eq. (7)

The analogous quantities are summarized below.

Electrical		Thermal	
Voltage	v	Temperature	θ
Current	i	Rate of heat flow	u
Electrical resistance	R_0	Thermal resistance	$1/\eta$
Electrical capacitance	C_0	Thermal capacitance	$c\rho$
Cylindrical coordinate	r, φ	Cylindrical coordinate	R, φ
Time	t	Time	τ

where γ = thermal conductivity of heat conducting medium
c = specific heat
ρ = density

The circuit shown in Fig. 4 may be regarded as the analog circuit of the two-dimensional heat conduction system.

Eq. (6) has as its solution

$$v(r, \varphi, t)=\sum_{m=0}^{\infty}\sum_{s=1}^{\infty} J_m(\lambda_{ms}r)\times(A_{ms}\cos m\varphi + B_{ms}\sin m\varphi)\,\varepsilon^{-\frac{\lambda^2_{ms}}{R_0C_0}t}+f(r, \varphi) \quad (8)$$

where A_{ms}, B_{ms}, λ_{ms} = constants determined by initial and boundary conditions
m, s = plus integer
$f(r, \varphi)$ = solution in steady state

$f(r, \varphi)$ is given by

$$f(r, \varphi)=\sum_{p=0}^{\infty} r^p(C_p\cos p\varphi + D_p\sin p\varphi) \quad (9)$$

where C_p, D_p = constants determind by boundary conditions
p = plus integer

If the results of the theoretical analysis for Eq. (8) coincide with the results obtained by the experimental analysis shown in Fig. 5 under the same conditions, the imaginary equivalent circuit shown in Fig. 4 can be regarded as the true equivalent circuit of the element. Consequently, the element can be utilized as the simulator of the two-dimensional heat conduction system.

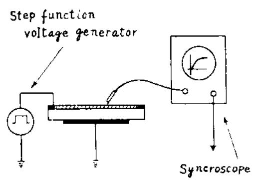

Eig. 5. The connection diagram for the experimental analysis

When an unit function voltage is applied between the circular electrode set up in $r=a$ and ground, the solution by the theoretical analysis is given by

$$v(r, t)=1-\frac{2}{a}\sum_{s=1}^{\infty}\frac{J_0(\lambda_{0s}r)}{\lambda_{0s}J_1(\lambda_{0s}a)}\,\varepsilon^{-\frac{\lambda^2_{0s}}{R_0C_0}t} \quad (10)$$

or $$v(r, t)\simeq 1-\frac{2}{a}\sum_{s=1}^{3}\frac{J_0(\lambda_{0s}r)}{\lambda_{0s}J_1(\lambda_{0s}a)}\,\varepsilon^{-\frac{\lambda^2_{0s}}{R_0C_0}t} \quad (11)$$

Since inserting the numerical values of constants in Table 2, the calculated results shown in Table 3 are obtained.

Table 2. Numerical values of constants

a	R_0	C_0	$\lambda_{01}\cdot a$	$\lambda_{02}\cdot a$	$\lambda_{03}\cdot a$
60mm	105 kΩ	26 pF/cm²	2.40	5.52	8.65

Table 3. Calculated values of the solution obtained by theoretical analysis

r \ t(μs)	0	5	10	20	30	50	100
a	1.00	1.00	1.00	1.00	1.00	1.00	1.00
3a/4	0	0.50	0.68	0.83	0.91	0.97	1.00
a/2	0	0.17	0.40	0.67	0.82	0.94	1.00
a/4	0	0.04	0.22	0.55	0.75	0.92	1.00
0	0	0.01	0.16	0.50	0.73	0.91	1.00

The experimental results for Fig. 5 is as shown in Fig. 6.

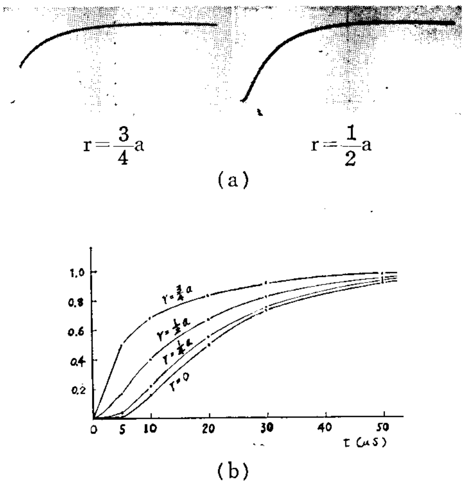

Fig. 6. The oscillograms obtained by the experimental analysis (a) and those copies (b)

Both results are coincident very well. So that the circuit shown in Fig. 3 can be represented by the element.

Comparing the wave forms in each point on the same circle, all of these are coincident. Therefore, the uniformity of the element for all direction is as expected.

§ 5. Practical setup procedure and applications for the transient heat conduction problems

As mentioned above, heat flow in two-dimensional fields is governed by Eq. (7). The scale factor N_v, the size ratio N_r and the time scale factor N_t are given by

$$N_v=\theta/v,\quad N_r=R/r,\quad N_t=\tau/t \qquad (12)$$

These equations are the relations describing the transformation from the original system variables to the element variables. Substituting Eq. (12) into Eq. (7)

$$\frac{1}{r}\frac{\partial}{\partial r}\left(r\frac{\partial v}{\partial r}\right)+\frac{1}{r^2}\frac{\partial^2 v}{\partial \varphi^2}=\frac{N_r^2}{N_t}\frac{c\rho}{\eta}\frac{\partial v}{\partial t} \qquad (13)$$

The follow equation must be established in order that Eq. (7) may coincide Eq. (6).

$$\frac{N_r^2}{N_t}\frac{c\rho}{\eta} = R_0C_0 \qquad (14)$$

Accordingly, the choice of R_0, C_0, or N_r and N_t are made so as to establish Eq. (14). So that the heat conduction problems can be analyzed by use of the RC distributed constant circuit, that is, the RC network element.

The following are the several problems of the transient heat conduction.

(Problem 1)

Determine the temperature distribution within the endless iron cylinder on which outer surface of $R=A=10\,cm$ the constant temerature is applied suddenly.

The magnitude of the physical constants are

$c = 0.108$ (*cal/g. deg*)
$\rho = 7.87$ (*g/cm*^{3})
$\eta = 0.18$ (*cal/cm. s. deg*)

Using the sample shown in Table 2, the values of the circuit constants of the element R_0, C_0 and the size ratio N_r are

$R_0 = 105$ ($k\Omega$)
$C_0 = 26$ (pF/cm^2)
$N_r = R/r = A/a = 1.67$

Substituting these values into Eq. (14), the time scale factor N_t is determined as follows.

$$N_t=\tau/t=\frac{N_r^2}{R_0C_0}\times\frac{c\rho}{\eta}=5.00\times 10^6$$

The connection diagram for the analog analysis of this problem is shown in Fig. 5. Imposing the step function voltage between the circular electrode set up in $r=a=6\,cm$ and ground, the oscillograms shown in Fig. 7 are obtained as the analog solutions. Transforming the scales to the original system, these oscillograms represent the temperature distribution within the iron cylinder.

The results of the theoretical analysis are

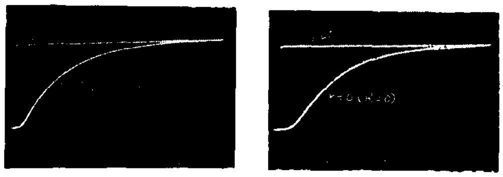

(a) (b)
HOR 50 SEC/CM

Fig. 7. The oscillograms obtained by the analog analysis (Problem 1)

$$\theta(R,\tau)=\theta_0\left(1-\frac{2}{A}\sum_{s=1}^{\infty}\frac{J_0(\lambda_{0s}R)}{\lambda_{s0}\cdot J_1(\lambda_{0s}A)}\varepsilon^{-\frac{\eta}{c\rho}\lambda_{0s}^2\tau}\right) \qquad (15)$$

where A = radius of iron cylinder

(Problem 2)

Determine the temperature distribution within the endless iron cylinder applied the constant temperature suddenly on the half surface covered from $\varphi=0$ to $\varphi=\pi$ and the ideal atomospheric temperature 0 on the other half surface. The magnitude of the physical constants c, ρ, η and the values of R_0, C_0, N_r and N_t are the same as those of problem 1.

The connection diagram is shown in Fig. 8 and the analog solutions are shown in Fig. 9. The results of the theoretical analysis are

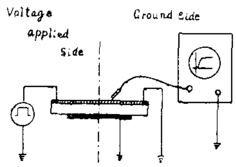

Fig. 8. The connection diagram for the analog analysis (Problem 2)

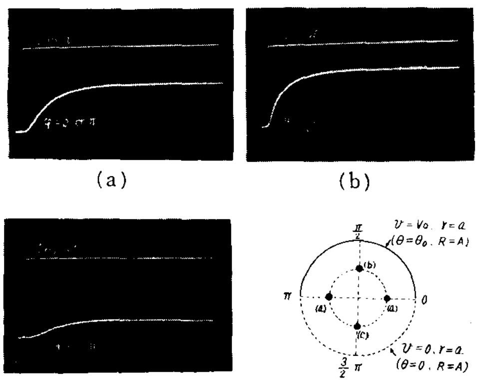

(a) (b)
(c) HOR 100 SEC/CM

Fig. 9. The oscillograms in $r=a/2$, (corresponded to $R=A/2$) obtained by the analog analysis (Problem 2)

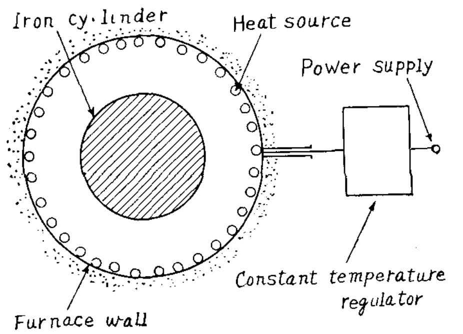

Fig. 10. A cross-scetional view of the endless iron cylinder in the furnace

$$\theta(R,\varphi,\tau)=\frac{\theta_0}{2}\left(1-\frac{2}{A}\sum_{s=1}^{\infty}\frac{J_0(\lambda_{0s}R)}{\lambda_{0s}J_1(\lambda_{0s}A)}\varepsilon^{-\frac{\eta}{c\rho}\lambda_{0s}^2\tau}\right)$$
$$+\frac{2}{\pi}\theta_0\left[\sum_{n=0}^{\infty}\frac{1}{(2n+1)}\left(\frac{R}{A}\right)^{2n+1}\sin(2n+1)\varphi\right.$$
$$\times\left\{1-\frac{2}{A}\sum_{s=1}^{\infty}\frac{J_{2n+1}(\lambda_{2n+1,s}R)}{\lambda_{2n+1,s}J_{2n+2}(\lambda_{2n+1}A)}\right.$$
$$\left.\left.\times\ \varepsilon^{-\frac{\eta}{c\rho}\lambda_{2n+1,s}^2\tau}\right\}\right] \tag{16}$$

(Problem 3)

Determine the temperature distribution of the endless iron cylinder in the furnace having the cross section shown in Fig. 10. This problem contains the heat conduction and radiation phenomena. It follows that the heat energy is radiated from the furnace wall to the iron cylinder surface and the temperature within the iron cylinder is risen gradually. The heat energy is radiated according to Stefan-Boltzmann's law.

And then the radiant heat flow U is given by

$$U=K(\theta_1^4-\theta_2^4)=U_1-U_2 \tag{17}$$

where Θ_1 = temperature of furnace wall in (^0K)
Θ_2 = temperature of iron cylinder surface in (^0K)
K = constant determined by Stefan-Boltzmann's constant and by geometrical shape and relative position of both surfaces

In this problem, the temperature of the furnace wall is kept constant by the regulator.

And then

Θ_1 = constant

so that Θ_1^4 = constant

The simulation of this heat flow system is as follows.

In the part of the iron cylinder, the magnitude of the physical constants c, ρ, η and the values R_0, C_0, N_r and N_t are the same as those of problem 1,

For the radiant heat flow part, the analogous quantities are summarized below.

Electrical	Thermal
Voltage V_1, V_2	Temperature Θ_1, Θ_2
Current I, I_1, I_2	Radiant heat flow U, U_1, U_2

where $I_1 = kV_1^4$ (is constant in this problem)
$I_2 = kV_2^4$
$I = k(V_1^4-V_2^4)$
k = constant corresponded to K

The current sources generated the current (I) can be accomplished with the vacuum tube circuit shown in Fig. 11 and the suitable amplifier.

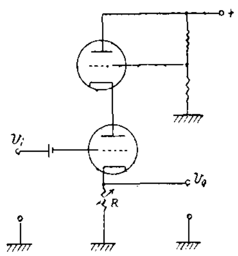

Fig. 11. A nonlinear element using the vacuum tube circuit

As shown in Fig. 12, in this vacuum tube circuit, the output voltage through the vacuum tube circuit v_0 is proportional to the input vol-

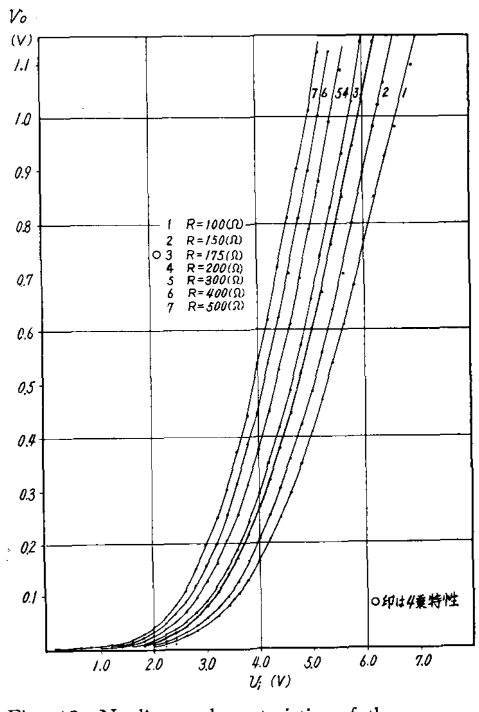

Fig. 12. Nonlinear characteristics of the vacuum tube circuit shown in Fig. 11

tage v_i raised to the fourth power.

The connection diagram of the analog system formed by the analogous current sources and the simulator of the iron cylinder is shown in Fig. 13.

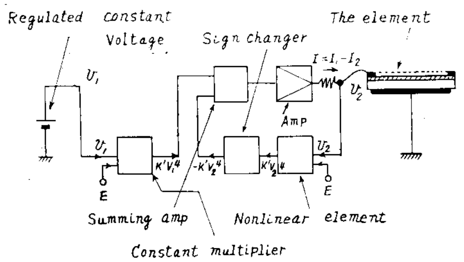

Fig. 13. The connection diagram for the analog analysis (Problem 3)

The oscillograms are shown in Fig. 14.

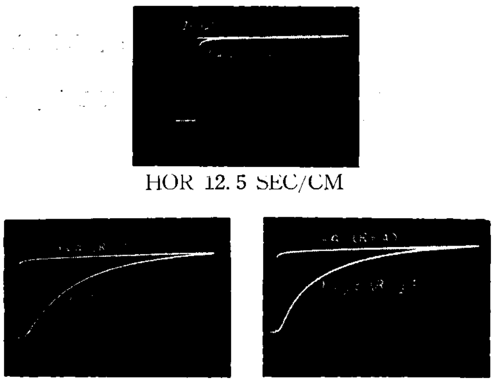

HOR 12.5 SEC/CM

HOR 50 SEC/CM

Fig. 14. The oscillograms obtained by the analog analysis (Problem 3)

(Accuracy check for problem 3)

The results of the numerical analysis obtained by use of the digital computer (NEAC 2203 made in Japan) are shown in Fig. 15 and in Table 4.

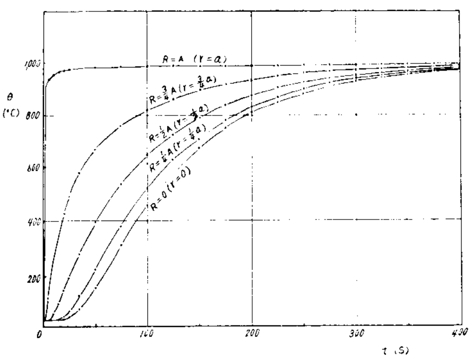

Fig. 15. The results of the numerical analysis obtained by use of the digital computer (NEAC 2203) (Problem 3)

Table 4. The printed data by the digital computer (NEAC 2203)

τ (s)	θ (deg)				
	R=A	3A/4	A/2	A/4	0
25	5397126	5349070	5318186	5262532	5233878
50	5398225	5366623	5339204	5321833	5314914
70	5398731	5375688	5353950	5338295	5331315
100	5399050	5381644	5364764	5352114	5346292
125	5399276	5385967	5372937	5363047	5358448
150	5399446	5389226	5379190	5371538	5367968
175	5399575	5391717	5383991	5378092	5375337
200	5399673	5393628	5387682	5383140	5381018
225	5399748	5395098	5390522	5387027	5385393
250	5399806	5396228	5392707	5390017	5388760
275	5399851	5397098	5394389	5392319	5391351
300	5399885	5397767	5395682	5394090	5393345
325	5399912	5398281	5396678	5395452	5394879
350	5399932	5398678	5397443	5396501	5396060
379	5399947	5398982	5398033	5397307	5396968
400	5399959	5399217	5398486	5397628	5397667
425	5399969	5399397	5398835	5398406	5398205
450	5399976	5399536	5899103	5698773	5398619
475	5399981	5399643	5399310	5399056	5398937
500	5399985	5399725	5399469	5399273	5399182
525	5399989	5399788	5399591	5399441	5399370
550	5399991	5399837	5399685	5399569	5399515
575	5399993	5399874	5399758	5399669	5399627
600	5399994	5399903	5399813	5399745	5399713
625	5399996	5399925	5399856	5399803	5399779
650	5399996	5399942	5399889	5399849	5399830
675	5399997	5399956	5399915	5899883	5399869
700	5399998	5399966	5399934	5399910	5399899
725	5399998	5399973	5399949	5399931	5399922
750	5399998	5399979	5399961	5399946	5399940
775	5399999	5399984	5399970	5399959	5399954
800	5399999	5399987	5399976	5399968	5399964
825	5399999	5399990	5399982	5399975	5399972
850	5399999	5399992	5399986	5399981	5399978
875	5399999	5399994	5399989	5399985	5399983
900	5399999	5399995	5399991	5399988	5399987
925	5399999	5399996	5399993	5399991	5399990
950	5399999	5389997	5399995	5399993	5399992
975	5399999	5399997	5399996	5399994	5399994
1000	5399999	5399998	5399996	5399995	5399995

53→$\times 10^{-2}$, 52→$\times 10^{-3}$, Example 5397126→971.26 (deg)

Taking a view of the results, such a direct analog method has not necessarily a high accuracy for these nonlinear problems, but has an allowable accuracy in practice (better than *3 per cent*). If better accuracy is required, it is desired to make use of the digital device for the nonlinear parts.

As it is often required the simplicity of the analysis rather than the high accuracy in engineering work, it may be estimated for the analysis of these nonlinear problems.

§ 6. Conclusion

It is well known that an analog method for the analysis of the transient phenomena is very effective. Here a simple and typical RC distributed circuit is represented, and it has an accuracy good enough for practical use. Also it is very convenient that the circuit constants are capable to vary by changing the thickness of the carbon film and the boundary conditions by repainting the shape of the silver electrode in accordance with the problems. The distributed variabe constants circuit can be represented by changing the dielectric thickness or the carbon film thickness.

As above, the design considerations and some applications of the RC distributed constants circuit, that is, the RC network elements are summarized, but for its application it is only described about few problems. From now on it must be established the application of the element.

The authors are grateful for the instruction received from Dr. Sigenori Hayashi, Prof. of Kyoto University, Dr. Kiyoshi Okazaki, Prof. of Defense Academy, Mr. Takashi Suzuki, Defense Agency, and for the useful suggestions given from the references (1), (2). Votes of thanks are also due to Mr. Kaoru Tomono and Miss. Ayako Ogasawara for their assistance in the experiments and the calculations.

References

1) W. J. Karplus: Analog Simulation (McGraw-Hill)
2) W. J. Ran: Control Eng. (1963 June) 85
3) T. Misaki, K. Okazaki: J. I. E. E. of Japan 80 (1960) 156.
4) T. Misaki, K. Okazaki, T. Suzuki: J. I. E. E. of Japan 80 (1960) 1426
5) K. Okazaki, T. Misaki, T. Yoshioka, Y. Yokoyama: J. I. E. E. of Japan (1961) 1779